

Transmission Analysis of Ring Resonator Based Optical Backplanes in high Capacity Routers



By

Mehmood Alam

A thesis submitted to the faculty of Electrical Engineering Department Military College of Signals, National University of Sciences and Technology, Rawalpindi in partial fulfillment of the requirements for the degree of MS in Electrical (Telecommunication) Engineering

September 2014

SUPERVISOR CERTIFICATE

It is certified that the final copy of the thesis has been evaluated by me, found as per format and error free.

Dr. Imran Rashid

ABSTRACT

Today's never ceasing thrust towards the achievement of greater aggregate bandwidth at lower cost has been completely steering the evolution of communication systems. Today's electronic backplane has many limitations such as power consumption and dissipation, power supply and footprint requirements. To cope with this high demand of greater bandwidth we need an architecture which implements optical switching without any need of Optoelectronic conversion. One of the proposed solutions is ring resonator based optical backplane [1] for router line card interconnection.

This research work presents a detailed performance analysis of the proposed architecture, considering all the real world parameters affecting the architecture such as number of line cards, switching-element round-trip losses, frequency drifting due to thermal variations and waveguide-crossing effects. In particular to quantify the signal distortions introduced by filtering operations, the bit error rate for the different parameter conditions are shown in case of an on-off keying non-return-to-zero input signal at 10 Gb/s.

DECLARATION

It is declared here that no portion of work presented in this thesis has been submitted in support of another award or qualification either in this institution or anywhere else.

DEDICATION

In the name of ALLAH, the most beneficent, the most merciful

Dedicated to my family, friends and teacher, without their help I would not be able to
complete this task

ACKNOWLEDGEMENTS

My first and foremost acknowledgements go to The Omnipotent, Almighty Allah whose exalted blessings flourished us thoughts and guided us in our endeavor to come up this manuscript as a representation of our effort which we undertook in past six months.

I also offer my humble thanks to Holy Prophet Muhammad (PBUH), the perfect Being, whose life is like a glowing candle; an everlastingly source of guidance for the entire humanity.

I am deeply indebted to my Parents and family for their utmost attention and efforts to make my study successful. I would also like to extend my gratitude for their continuous moral support and devoted prayers, which keep my spirits high for the daunting tasks of life and without whom it would have been hard for us to realize the true essence of life.

Many people have contributed to the development of this project. I am really grateful to my Supervisor Dr. Imran Rashid for his guidance and cooperation throughout the research period. Special Thanks to Dr. Maurizio Magarini from PLOMI, Italy for his great help and support which makes this research work possible within due time.

I thank Dr. Abdul Rauf, Dr. Adil Masood Siddiqui and Lt. Col. Umer Khalid for agreeing on my thesis committee and providing me the feedback

Finally, I would like to appreciate all those who helped and encouraged me in making this job successful.

TABLE OF CONTENTS

<i>Chapter 1</i>	8
INTRODUCTION	8
1.1 Overview	8
1.2 High Performance Switches and Routers.....	9
1.3 Why Optical Backplanes?.....	9
1.4 Optical Interconnection Architecture	10
1.5 Single Plane Scenario	10
1.6 Multi Plan Scenario.....	10
1.7 Working Principle	11
1.8 Summary	12
<i>C H A P T E R 2</i>	13
Signal to Noise Ratio and Bit Error Rate.....	13
2.1 Introduction.....	13
2.2 Optical Receiver Model.....	13
2.3 Optical Signal to Noise Ratio (OSNR)	13
2.4 Electrical SNR	14
2.5 Relation between OSNR and SNR.....	15
2.6 Bit Error Rate Evaluation.....	15
2.7 Bit Error Rate.....	15
2.8 BER Performance Analysis	16
2.9 Eye Diagram	17
2.10 Receiver Model.....	18
2.11 Binary Antipodal Transmission	19
2.12 Optical Fiber Transmission.....	20
2.13 Equivalent Receiver Model.....	21
2.14 Q-Factor	22
2.15 Summary	25
<i>Chapter 3</i>	27
ASE Noise, inter-channel Interference and Photodetector Noise	27
3.1 Introduction.....	27
3.2 ASE Noise.....	27
3.3 EDFA Working Principle.....	27
3.4 Amplifier Spontaneous Emission (ASE) Noise	28

3.5	Effect of ASE Noise on BER.....	29
3.6	Simulation Parameters	30
3.7	Simulation Results	30
3.8	Inter-Channel Interference (ICI)	31
3.9	ICI Effect	31
3.10	ICI effect on BER Performance	32
3.11	Photodetector Effect.....	34
3.12	Summary	37
<i>Chapter 4</i>		38
Temperature, Round trip Loss and Channel Spacing.....		38
4.1	Introduction	38
4.2	16 Channels at 50 GHz Spacing	38
4.3	64 Channels at 25 GHz Spacing	39
4.4	Channel spacing Comparison.....	40
4.5	Effect of Temperature	42
4.6	Round trip Loss.....	44
4.7	Summary	46
Conclusion and Future Work		47
References.....		48

LIST OF FIGURES

Figure 1.5-1.5-1: Single Plane Scenario.....	10
Figure 1.6-1: OI Architecture	11
Figure 1.7-1: Drop port Transfer Functions at different stages	12
Figure 3.3-1: BER Evaluation schematic.....	16
Figure 3.3-2: Pulse	17
Figure 3.4-1: Eye Diagram	18
Figure 3.6-1: Receiver model BPSK	20
Figure 3.7-1: Optical fiber Receiver model	21
Figure 3.8-1: Equivalent Receiver Model	22
Figure 3.9-1: Comparison between exact and approximated threshold	24
Figure 3.9-2: Eye Diagram- Q-factor Extraction	25
Figure 4.3-1: EDFA Working Principle	28
Figure 4.4-1: ASE noise.....	28
Figure 4.5-1: BER Evaluation Schematic (EDFA Noise).....	29
Figure 4.7-1: BER vs. SNR plot for all 32 channels at 50 GHz Spacing.....	30
Figure 4.7-2: BER VS SNR - Best, Worst and Average Channels	31
Figure 4.9-1: Inter-Channel interference	32
Figure 4.10-1: BER VS SNR - ICI effect.....	33
Figure 4.10-2: BER Performance comparison-With and Without ICI.....	34
Figure 4.11-1: Photodetector Equivalent Model	35
Figure 4.11-2: BER evaluation Schematic-Photodetector noise effect.....	36
Figure 4.11-3: BER VS SNR – Overall architecture	37
Figure 5.2-1: BER VS SNR plot for 16 channels at 100 GHz spacing.....	39
Figure 5.3-1: BER VS SNR plot case for 64 channels at 25 GHz spacing.....	40
Figure 5.4-1: Comparison of 25, 50 and 100GHz channel spacing without Photodetector noise.....	41
Figure 5.4-2: Comparison of 25, 50 and 100GHz channel spacing with Photodetector noise	42
Figure 5.5-1: BER vs. SNR- Temperature Effect.....	43
Figure 5.6-1: BER vs. SNR for transmission at 10 Gb/s of 32 NRZ-OOK channels with increasing round-trip losses $\alpha = 0, 0.2, 0.4, 0.6, 0.8, 1$	44
Figure 5.6-2: BER vs. SNR for transmission at 10 Gb/s of 32 NRZ-OOK channels with increasing round-trip losses $\alpha = 0, 0.2, 0.4, 0.6, 0.8, 1$ in presence of XT	45

INTRODUCTION

1.1 Overview

The rapid advancement in the field of telecommunication has converted the modern world into a global village. This advancement incredibly increased the traffic over the telecommunication networks which results into high demand for the greater bandwidth at lower cost. Unfortunately the current electronic backplanes have many limitations and thus is not a good candidate to meet this high demand projection.

To address this this high traffic growth rate projection the use of High Performance Switches and Routers (HSPRs) which are capable of managing huge aggregated bandwidth is mandatory [2]. The aim of the research work is to perform a detailed investigation of the transmission analysis of an architecture used in HSPRs taking into account all the parameters which can affect the performance such as

1. Attenuation
2. Temperature
3. Noise due to EDFA
4. Inter channel Interference
5. Noise due to Photo detector
6. Variation in channel spacing

This thesis report is organized as follows: The first chapter is the introduction of the research work and a brief overview of the architecture to be analyzed. Chapter 2 deals with the mathematical derivation of the Q factor. Chapter 3 is about the basic ideal communication model. Chapter 4 presents the effect of Noise and Inter channel interference on performance. Chapter 5 describes the variation in BER due to change in Temperature, Attenuation and channel spacing. Chapter 6 presents the analysis of the real world communication model.

1.2 High Performance Switches and Routers

A HPSR is commonly composed by one or more racks. Each rack contains a set of multiple carrier modules (cards) which are connected via a backplane [3][4]. Carrier modules can be divided into two types: line cards and control-logic cards. Line cards host the network interfaces (transmitters and receivers) and implement low-layer network-processing functions. In order to interconnect a large number of line cards the designer may choose between centralized and distributed approaches. Centralized switching is implemented by an all-electronic switching fabric hosted in a dedicated control logic card. In this case the backplane is a simple passive bus, whereas in distributed switching, the backplane itself performs the switching function (switching backplane). In such a context, different optical solutions are available to implement a switching backplane subsystem with the objective of achieving the aforementioned performance goals.

1.3 Why Optical Backplanes?

There are many reasons to choose Optical backplanes in HSPRs instead of Electronic backplanes. In high-performance network equipment the number of hardware modules to be interconnected tends to increase enormously as the interconnection data-speed scales up [5]. Today's majority of systems on the market adopt electrical wiring and electronics as interconnection technology and the simple bus as backplane architecture. Conventional electronic has a fundamental drawback in broadband transmission: the high-frequency components of the signal are attenuated due to increased conductor resistance in the high frequency region, and also cable material degrades the signal intensity as frequency increases.

Optical Interconnection (OI) represents a powerful alternative. Attenuation is frequency independent, i.e. it does not increase at high bit-rates. Optical transmission lines do not suffer the crosstalk impairment, though some optical crosstalk may occur inside the photonic devices. Several photonic functional blocks and devices are today available, even to realize complex-topology backplanes. OI has a wide range of application. OI can be deployed between racks (rack-to-rack), between line-cards inside a rack (card-to card or backplane), between chips of a line-card (chip-to-chip), or even between the different cores of a single chip (on-chip). Obviously, by changing the size and the characteristics of the problem different solutions to a various range of issues may be studied.

This research work focus on the card to card Optical Interconnection. In which a detailed transmission analysis has been done in terms of Bit Error Rate (BER).

1.4 Optical Interconnection Architecture

In this section the ring resonator based switching backplane is discussed along with description of the design procedure for routing assignment in this architecture.

1.5 Single Plane Scenario

Following is the basic single plane scenario of the communication system in which N line cards are on the same selection circuit on both sides. On left side there are N transmitters while on right side N receivers are connected. From each transmitter it is possible to reach any receiver. Routing between input and outputs is controlled through wavelength selection at transmitters.



Figure 1.5-1 Single Plane Scenario

1.6 Multi Plan Scenario

In Multiplan scenario the switching fabric is divided into S planes and accordingly the N line cards are divided in subsets of N/S elements. Each subset is connected to one of the S switching fabric.

Our research work is based on the switching backplane represented in Fig.1.6-1. A Binary-Tree Ring Router (BTRR) used to select the output plane represents the plane selection circuit whereas a ring resonator array demultiplexer represents the receiver selection circuit. In this architecture only point-to-point connections have to be established between TXs and RXs, with no output contention, i.e. each RX is to be connected to at most one TX using one single wavelength.

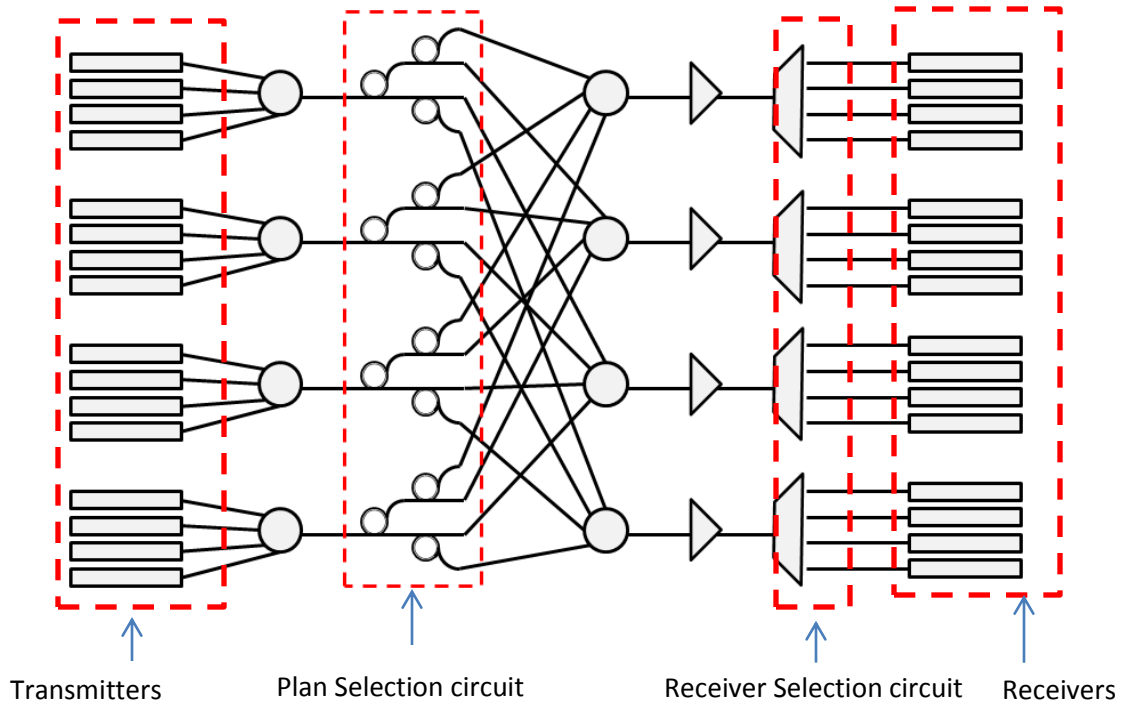


Figure 1.6-1: OI Architecture

1.7 Working Principle

The principle of the tree-structure ring resonator plane selection circuit is the same of that based on a cascade of Mach-Zehnder filters, the so-called interleaving. An interleaver is a multi-stage demultiplexer with T stages where at each stage each ring resonator spatially discriminates the incoming wavelength-channels partitioning them into two alternate subgroups, sending half of them towards the “through” port and half of them towards the “drop” port. T has to be large enough to completely discriminate all the S switching planes, i.e. rings of the last stage separate only two channels: therefore $T = \lceil \log_2(S) \rceil$. The j th stage will be composed of $2^{(j-1)}$ ring resonators, with $1 \leq j \leq T$ and after j stages 2^j planes can be selected. To fulfill these requirements, each ring of the j th stage has to be designed with a free spectral range (FSR), centered on the first incoming wavelength, such that $FSR_j = 2^j \Delta\lambda$.

Figure 1.7-1 shows general ring drop port transfer function before 1st stage, after first stage and after second stage respectively.

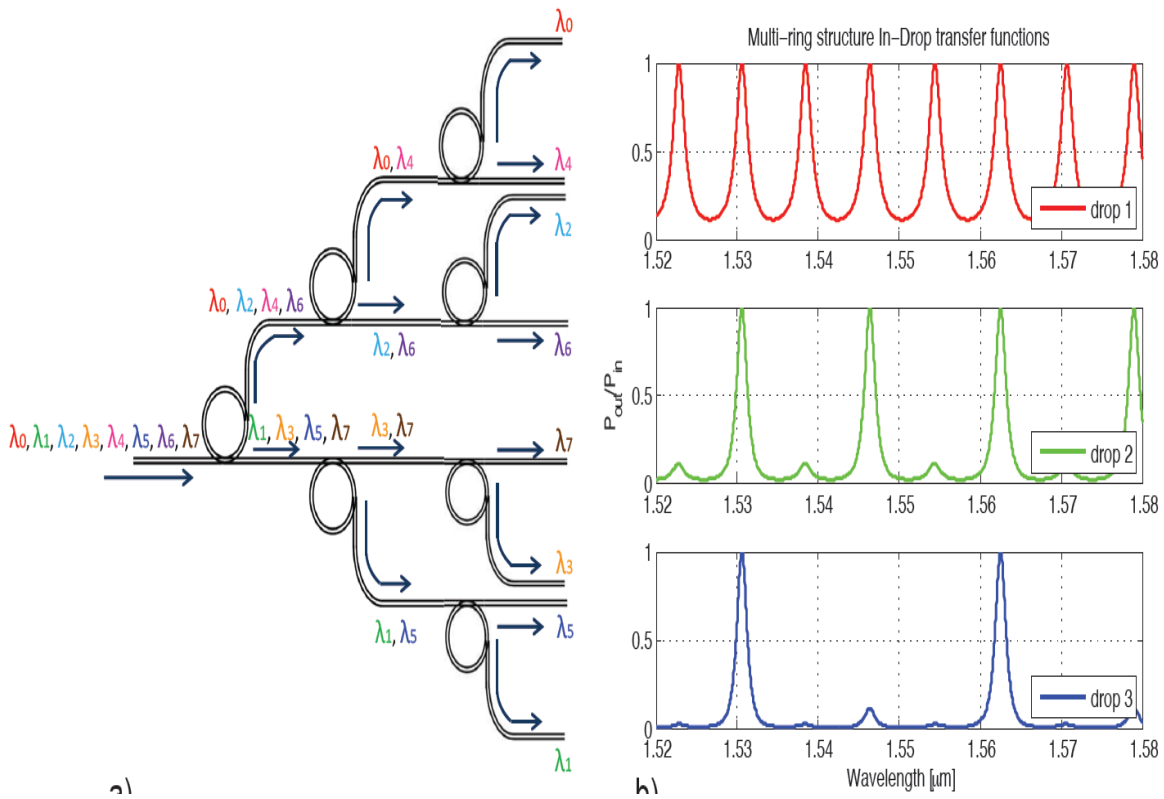


Figure 1.7-1: Drop port Transfer Functions at different stage

1.8 Summary

In this chapter a brief introduction of the research work and literature review has been discussed in detail. The objectives of the thesis have been elaborated. It has been highlighted that why optical backplanes are preferred over electronic backplanes in high capacity switches and routers. The architecture and working principle of the ring resonator based optical backplane has been studied.

Signal to Noise Ratio and Bit Error Rate

2.1 Introduction

Modern high speed transmission use optical fiber as a medium of information transportation due to its higher data rate and advantages over electronic transmission as discussed before. But even these excellent transmission media are subject to noise, distortion and dispersion of the signal, especially if used for the transmission in WDM (Wavelength Division Multiplexing).

For an optical communication system to achieve a given Bit error rate (BER), a minimum average signal power must be received at the receiver [6]. The ratio of signal power to noise power at the receiver of a fiber-optic communication system has a direct impact on the system performance. In order to accurately demodulate the signal, it is important that signal power be large in comparison to the noise power. This ratio is called signal to noise ratio (SNR). Knowledge of the ratio of the signal power to the noise power (signal-to-noise ratio or SNR) is important because it is directly related to the bit error ratio (BER) in digital communication systems, and the BER is a major indicator of the quality of the overall system [7].

2.2 Optical Receiver Model

In Optical communication system the signals are ideally represented by a pulse of light or absence of light. During transmission noise superimposed on this which can be considered as White Gaussian Noise (WGN) or Amplifier Spontaneous Noise (ASE), as the noise in optical fiber communication system is introduced by the spontaneous emission of the optical Amplifier. The model that describes the optical receiver we have used is ON/OFF Keying (OOK) i.e. a binary 1 is represented by a pulse of light and 0 is represented by absence of pulse.

Following is a brief overview of the electrical and optical SNR and the relationship between them.

2.3 Optical Signal to Noise Ratio (OSNR)

OSNR is defined as the ratio of the average optical power of the signal to the total noise power. Mathematically Optical SNR can be expressed as [8]

$$OSNR = \frac{P}{N_{ASE}B_{ref}} \quad (1)$$

Where:

- P = Total average signal power summed over the two states of polarization
- N_{ASE} = Spectral density of amplified spontaneous emission
- B_{ref} = Reference Bandwidth

The factor 2 is normally used for considering both polarizations of ASE.

2.4 Electrical SNR

Electrical SNR is defined as

$$SNR = \frac{E}{N_0}$$

Where E is the Energy of the signal and N_0 is the Noise spectral density

As

$$E = \frac{P}{R_s}$$

R_s is the Symbol Rate and P is Power of the signal

$$SNR = \frac{P}{N_0 R_s} \quad (2)$$

As we have different number of bits per symbol for different modulation schemes, so to compare different types of modulation formats, we need SNR which should be based on energy per bit unlike the SNR which is based on energy symbol.

Thus we define SNR_b as the energy per bit as follows

$$SNR_b = \frac{SNR}{\tilde{R}}$$

\tilde{R} is the number of information bits per modulation symbol.

SNR_b is often denoted as E_b/N_0 as the energy per information bit is $E_b = E/\tilde{R}$.

In our scenario the electrical SNR is given by the ratio of the signal power and noise power after electrical filtering with the same bandwidth as that of the Plan Selection Circuit (PSC)

2.5 Relation between OSNR and SNR

The OSNR and electrical SNR can be compared as follows:

From eq (1) and (2)

$$OSNR = \frac{pR_s}{2B_{ref}} SNR$$

Where

$$p = 1 \text{ for single polarized signal}$$

As the ASE noise contributes only over the receiver bandwidth which is narrower than bandwidth of the filter, the electrical SNR is higher than the Optical SNR.

2.6 Bit Error Rate Evaluation

Instead of the traditional method of finding the BER, a semi analytical approach was followed for finding the Bit Error Rate (BER) which has been explained in the upcoming sections of this chapter.

In conventional method of BER evaluation the received bit sequence is examined to find the number of bits in error and then compared with the original transmitted sequence. This method is very much time consuming and also is high computational power demanding.

2.7 Bit Error Rate

Bit error rate is the widely used measure of the overall system performance. It is defined as the ratio of the total number of bits in error to the total number of transmitted bits. It actually gives an idea of the bits which are flipped from 1 to 0 or vice versa while passing through the different components between the transmitter and receiver.

In the following section, a semi analytical approach will be followed to determine an expression for evaluating the BER for the ring resonator based optical backplane architecture.

2.8 BER Performance Analysis

For this specific case the transmission at 10 GB/s of 32 OOK-NRZ signals which are spaced at 50 GHz is considered.

The following schematic in fig 3.3-1 shows the flow of signal through different section of the architecture.

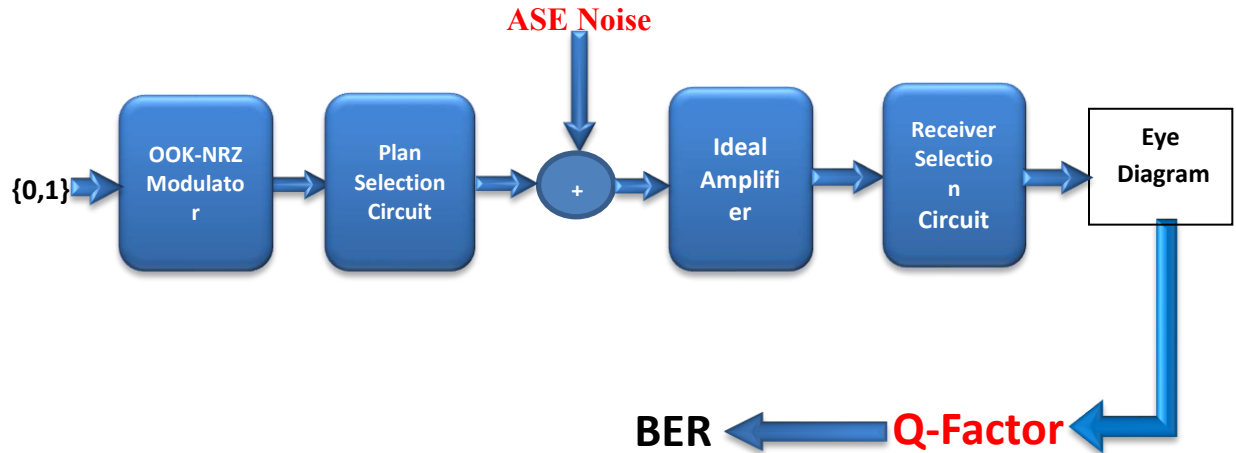


Figure 2.8-1: BER Evaluation schematic

10 Gb/s signal is introduced into the NRZ-OOK Modulator Which modulate the input bits {0,1} into pulse of amplitude 0 and 1 i.e. when the input bit is 1 the NRZ-OOK modulator outputs the signal into a pulse of amplitude 1 and for the case of 0 input the modulator output is zero .

For performance analysis the impulse response used for pulse shaping was chosen with a rise and fall time of 35% the bit duration as shown in the figure 3.3-2. As in real case an ideal pulse shaping filter of zero rise and fall time is impossible, thus the said value was selected to make the system closer to real world scenario.

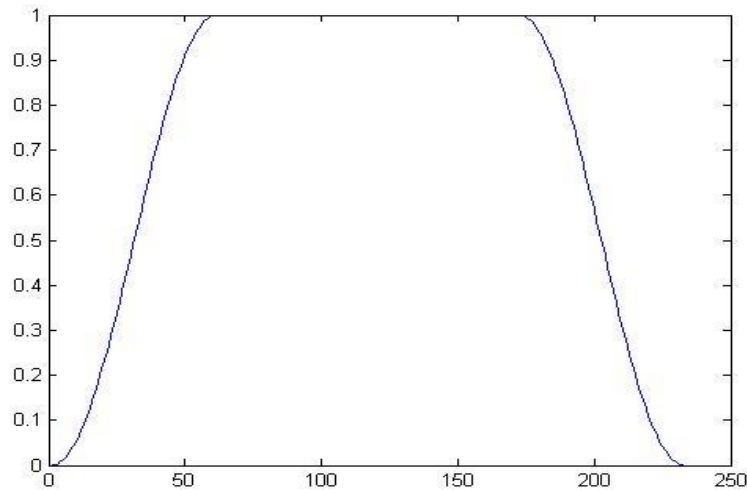


Figure 2.8-2: Pulse

After passing through the pulse shaping filter the signal is passed through the plan selection circuit which is basically the transfer function or impulse response of the channel.

Erbium Doped Fiber Amplifier (EDFA) is modeled as a source of white Gaussian noise which is the Amplifier Spontaneous Noise (ASE noise) and an ideal amplifier. The effect and origin of this noise will be discussed latter in next chapters of this report. The signal is then introduced into a Receiver the Selection Circuit (RSC) filter and then the Photodetector which finally converts the signal into binary ones and zeros.

As certain filtering operations have been performed on the signal by PSC and the RSC filters, due to which some dissipation is introduced in the signal. This effect of filtering operations performed by a certain TX-RX pair on the input signal and the resulting distortions can be estimated by means of the eye diagram [9].

By investigating the eye diagram the Q factor is extracted which ultimately leads to the Bit Error Rate (BER).

2.9 Eye Diagram

In today's high speed communication systems, the data is transmitted at Gigahertz frequencies. At higher frequencies the probability of signal degradation due to various parameters like transmission-line effects, impedance mismatches, signal routing, termination schemes, and grounding schemes increases. The signal is also degraded by impairments between transmitter

and receiver. Also the interference due to cables, PCB traces, connectors, and transmitter, affects the signal integrity. To inspect and analyze the integrity of the signal as early as possible, eye diagram is used as a tool.

Eye diagram is a measure of the signal quality. It is generated by repeatedly overlaying the segments of the long stream of data [10]. The eye diagram thus generated contains all the possible bit sequences of 1s and 0s. The resulting image looks like an opening eye, thus the name eye diagram.

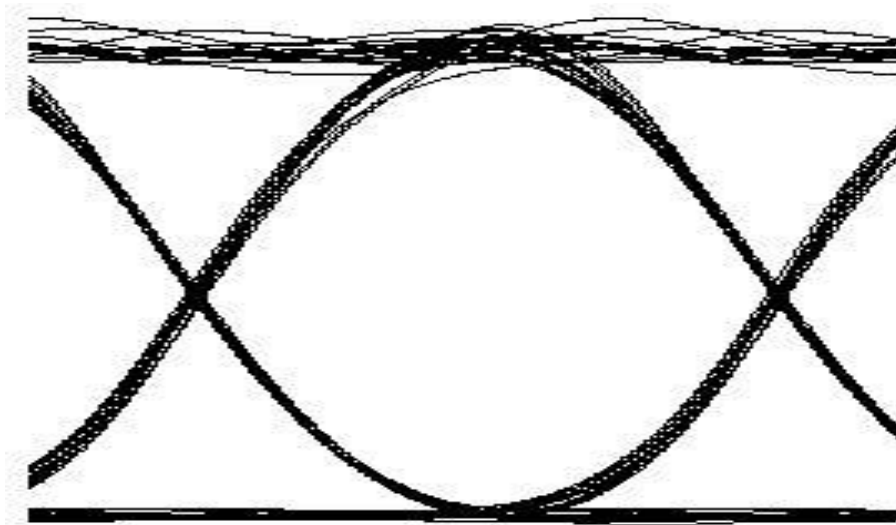


Figure 2.9-1: Eye Diagram

From the eye diagram, the Q factor is extracted by using the following procedure. The Q-factor is then used for the estimation of bit Error Rate.

2.10 Receiver Model

The modern high speed transmission systems use optical fiber for transfer of information. Even these excellent transmission media are subject to noise, distortion and dispersion of the signal, especially if used for the transmission in WDM (Wavelength Division Multiplexing). The signals in optical fiber are represented ideally with pulse of light or absence of light, to which is superimposed a noise which can be considered Gaussian. The model that describes the transmission in optical fiber is the type on / off. The model of the receiver is binary antipodal, that is well suited to the transmission power and in any case is can be considered as symmetrical.

Starting from the model of the receiver the binary antipodal will be introduced in the optical model of type On / Off and will describe and analyze the approximations through which one can switch from the second to the first model.

2.11 Binary Antipodal Transmission

Consider a channel used for transmitting binary antipodal; subject to a Gaussian noise with zero mean and variance $\sigma^2 = \frac{N_0}{2}$, Where N_0 is the noise spectral density. If we denote $E_s = E_b$, the energy transmitted per symbol, the distance between the two signals antipodal $+m$ and $-m$ appears to be:

$$d = \sqrt{E_b}$$

Assuming that the decision threshold of the receiver is positioned in $x = 0$, there exists equal probability of a wrong decision, which can be expressed as:

$$P(E) = Q\left(\frac{d/2}{\sqrt{N_0/2}}\right) = Q\left(\sqrt{E_b/N_0}\right)$$

Where the function $Q(x)$ is the Gaussian distribution and is given by

$$Q(x) = \frac{1}{2\pi} \int_x^{+\infty} \exp\left(-\frac{t^2}{2}\right) dt = \frac{1}{2} \operatorname{erfc}\left(\frac{x}{\sqrt{2}}\right)$$

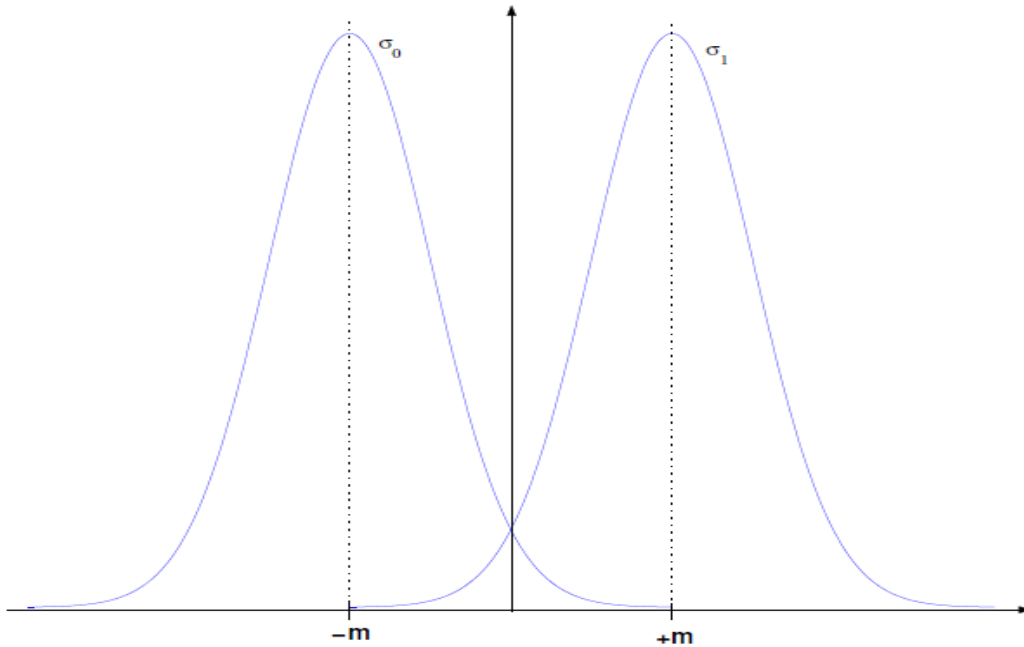


Figure 2.11-1: Receiver model BPSK

Figure 6 shows the receiver model of BPSK scheme. In which the point of intersection of the two curves for binary 0 and binary 1 lies at the 0.

Erfc(x) is the error function and is given by the equation:

$$erfc(x) = \frac{1}{\sqrt{\pi}} \int_x^{+\infty} \exp(-t^2) dt$$

2.12 Optical Fiber Transmission

In optical fiber transmission the optical power of the signal is associated with the source of information. Typically a positive bit is represented by a light pulse and a negative bit by absence of light, corresponding to on/off transmission model. Even the best optical fiber transmission systems suffer from dark currents and dispersions. In practice there are a few photons which affect the Photodetector.

Fig 3.7-1 represents the optical receiver model. Due to the imperfections in the system's transmission-reception, the signal that should have zero amplitude corresponds to an average value ρ . The standard deviation σ_0 is very low to move the threshold decision. Clearly the negative values have no effect and the distribution of noise would not be purely Gaussian.

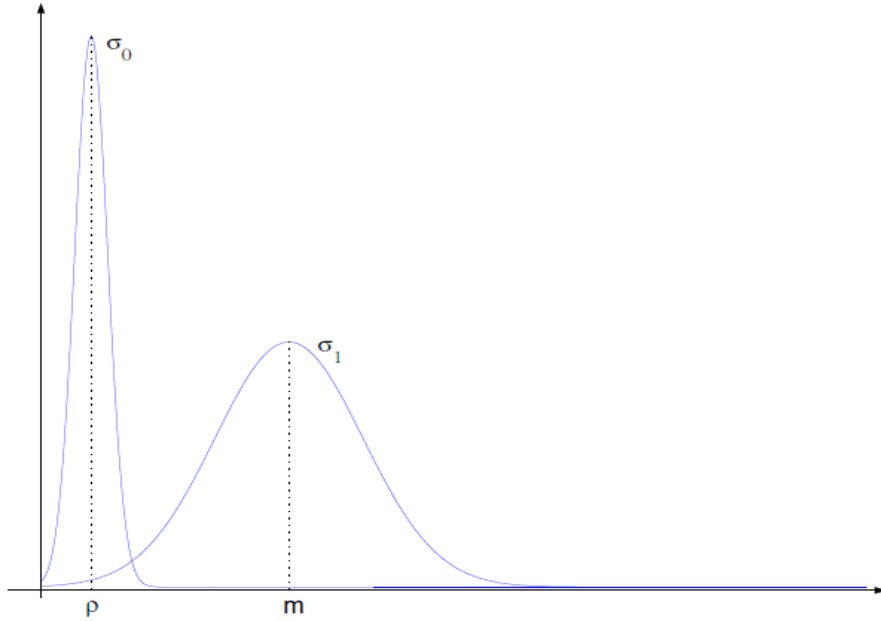


Figure 2.12-1: Optical fiber Receiver model

2.13 Equivalent Receiver Model

By translation and dilation it is always possible to transform a model such as that of Figure 3.7-1 into an equivalent model with the antipodal average value in zero.

Denoting the signal amplitudes by m'_0 and m'_1 and the associated standard deviations of noises by σ'_0 and σ'_1 , the equations that describe the transformation are

$$x = \left(x' - \frac{m'_0 + m'_1}{2} \right) \cdot \left(\frac{2}{m'_1 - m'_0} \right)$$

$$\sigma_0 = \sigma'_0 \frac{2}{(m'_1 - m'_0)} ; \quad \sigma_1 = \sigma'_1 \frac{2}{(m'_1 - m'_0)}$$

The antipodal model is preferred to use even if the transmission is on/off keying. It allows us to treat the two signals in the same way. Also the symmetry makes it easy to compare the signals directly with other models.

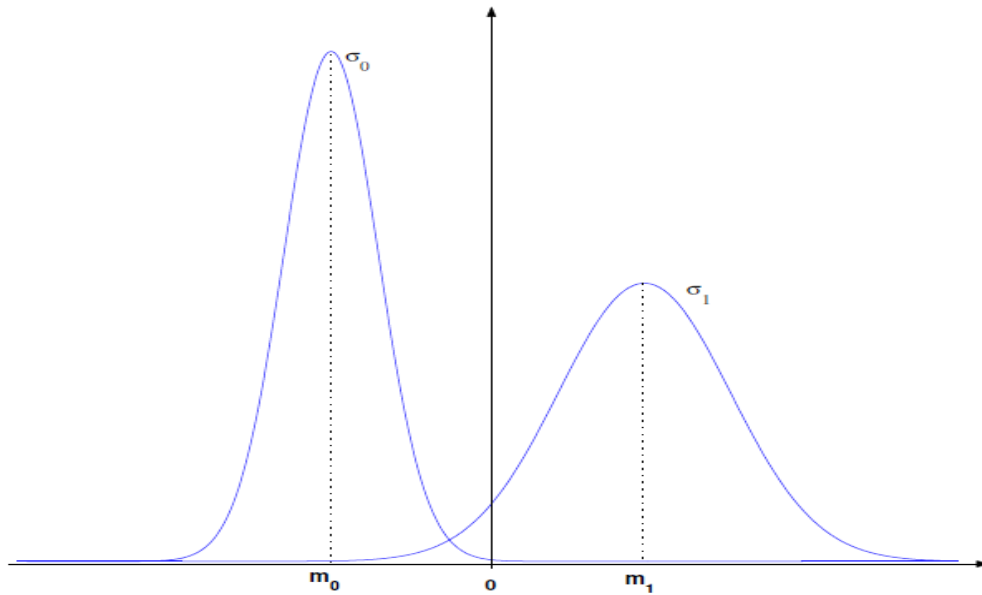


Figure 2.13-1: Equivalent Receiver Model

2.14 Q-Factor

Q-factor is an appropriate measure of the performance of the overall system. It gives an idea of how much the system is reliable in its performance. It is proportional to the system's SNR, Thus an increase in the SNR leads to an increase in the Q-factor [11]. Higher the Q-factor, better the quality of the signal will be.

In order to evaluate the Q-factor in the architecture under consideration, we consider the case where the detected signal is dominated by the thermal noise in the Photodetector.

Consider the model of the receiver for the transmission on/off keying model of figure 3.7-1, the position of the decision threshold would be at the intersection of the two Gaussians, which is the minimum sum of the areas of the two Gaussians. To find the exact position of the threshold the following equations must therefore be solved:

$$\frac{1}{\sqrt{2\pi\sigma_1^2}} e^{-\frac{(x-m_1)^2}{2\sigma_1^2}} = \frac{1}{\sqrt{2\pi\sigma_0^2}} e^{-\frac{(x-m_0)^2}{2\sigma_0^2}}$$

Which gives,

$$x_s = \frac{m_0\sigma_1^2 - m_1\sigma_0^2 - \sigma_1\sigma_0 \sqrt{(m_0-m_1)^2 - 2(\sigma_1^2 - \sigma_0^2) \ln \frac{\sigma_0}{\sigma_1}}}{(\sigma_1^2 - \sigma_0^2)}$$

For small values of σ_0 and σ_1 , x_s can be approximated as

$$x_s \cong \frac{m_0\sigma_1^2 - m_1\sigma_0^2 - \sigma_1\sigma_0(m_0-m_1)}{(\sigma_1^2 - \sigma_0^2)} = \frac{(m_0m_1 + m_1m_0)}{(\sigma_1 + \sigma_0)}$$

The approximation made is equivalent to consider as a threshold point where the area of the two tails equal, and slightly away from the intersection of the exact Gaussian.

Figure 3.9-1 shows the approximation and the exact threshold for different values of k. For small values of σ_0 and σ_1 in the above equation of x_s , their difference tends to zero.

The probability of error is then given by:

$$P(E) = \frac{1}{2}Q\left(\frac{m_1 - x_s}{\sigma_1}\right) + \frac{1}{2}Q\left(\frac{x_s - m_0}{\sigma_0}\right) = Q\left(\frac{m_1 - m_0}{\sigma_1 + \sigma_0}\right)$$

$$P(E) = Q\left(\frac{m_1 - m_0}{\sigma_1 + \sigma_0}\right)$$

The term $\frac{m_1 - m_0}{\sigma_1 + \sigma_0}$ is called the Q-factor

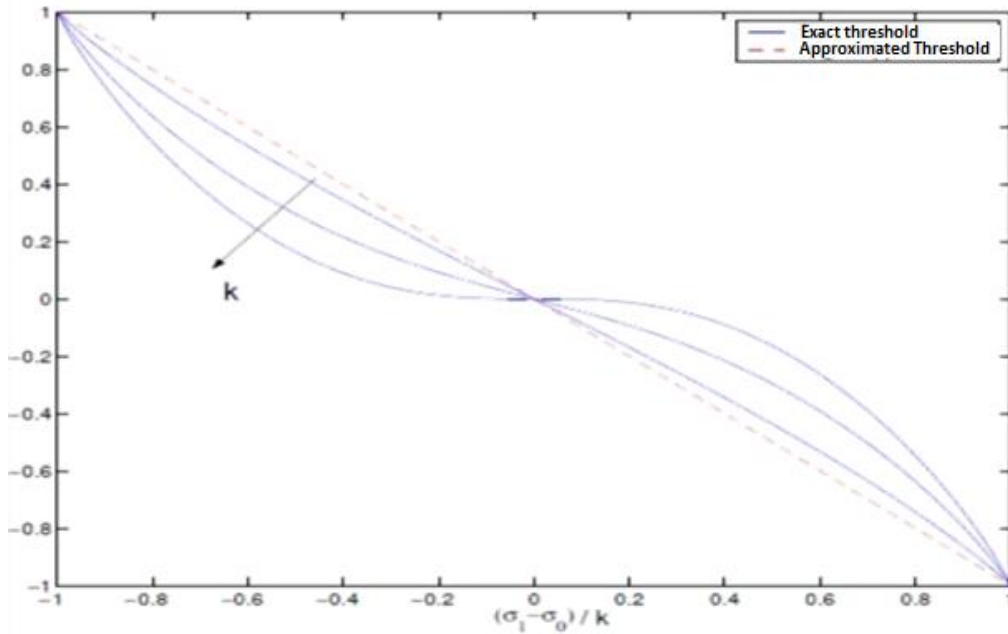


Figure 2.14-1: Comparison between exact and approximated threshold

Now as the term Q- factor has been evaluated, the value of this term is extracted from the eye diagram of the signal for the ring resonator based optical backplane for finding the overall BER.

The variables used in this equation can be related to the eye diagram shown in figure 3.9-2 as follows

m_0 : Mean value of '0' at maximum eye opening

m_1 : Mean value of '1' at maximum eye opening

σ_0 : Effective Standard deviation of 'zeros' distribution.

σ_1 : Effective Standard deviation of 'ones' distribution .

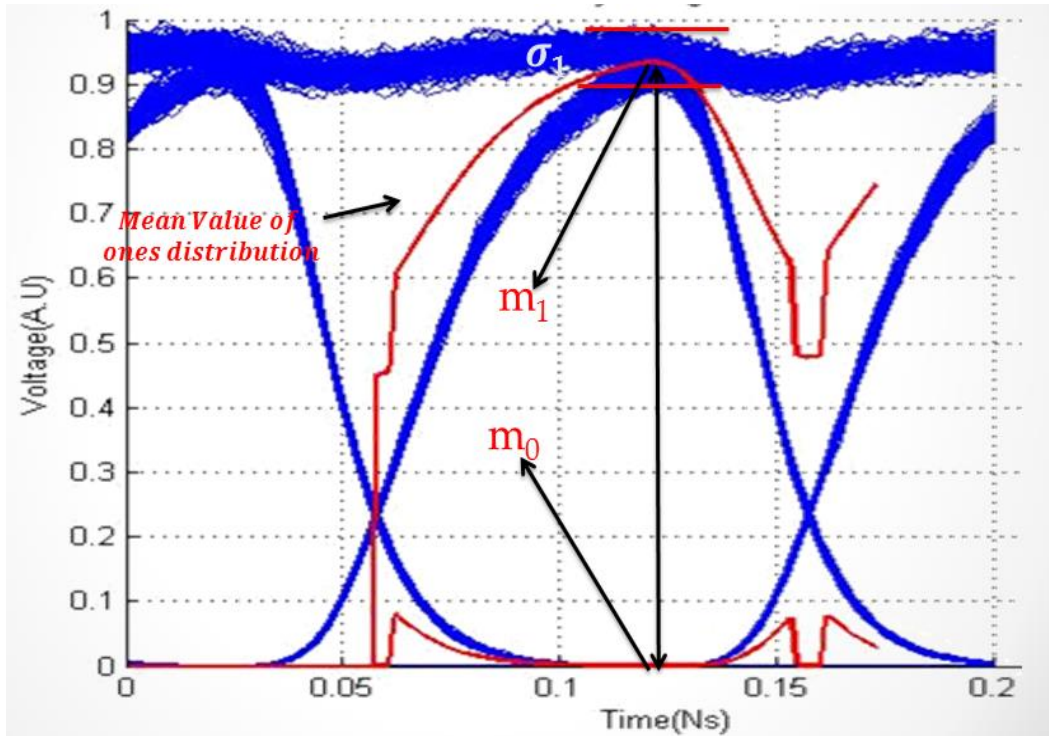


Figure 2.14-2: Eye Diagram- Q-factor Extraction

The BER is found by using the equation:

$$BER_{sim} = 0.5 * erfc\left(\frac{Q}{\sqrt{2}}\right)$$

Where Q is given by:

$$Q = \frac{m_1 - m_0}{\sigma_1 + \sigma_0}$$

2.15 Summary

This is the main chapter of the thesis which deals mainly with detail discussion of the Bit Error Rate extraction from the simulated eye diagram. A schematic of the BER evaluation process has been discussed in detail which shows an empirical image of the stages through which the signal passes like source, transmitter, plane selection circuit, receiver selection circuit etc. It also

elaborates that how and at which stage the EDFA noise has been introduced in system. Mathematical analysis of the Q factor has been given in detail. This chapter also presents an overview of the Signal to noise ratio for both optical and electrical domain and also presents the relation between them.

ASE Noise, inter-channel Interference and Photodetector Noise

3.1 Introduction

Noise is defined as the source of making the original signal deviate from its original form. It is usually associated with random processes. Noise corrupts the information content and fidelity of the signal. In this chapter the effect of noise which originates from different sources like the Amplifier Spontaneous Emission (ASE) noise, Inter-channel interference and noise originated due to the Photodetector will be discussed. The distortion caused by these sources will be investigated, which leads to the degradation of the signal and finally degrade the Bit Error Rate performance.

3.2 ASE Noise

In optical fiber transmission line the signal is degraded by three basic noise sources i.e. Fiber loss, Dispersion and Non Linear Effects. As these sources are unavoidable and have specific values for each fiber type, we must compensate these effects by introducing different techniques. The most used and effective of which are the use of optical amplifier and dispersion management. As the receiver can only detect the signal which has power above some threshold, the amplifier compensates the signal power attenuation. The receiver then can easily detect the signal. For this optical system Erbium Doped Fiber Amplifier (EDFA) has been used.

3.3 EDFA Working Principle

EDFA are preferred over semiconductor fiber amplifiers due to its advantages over semiconductor amplifiers like polarization sensitivity, inter channel crosstalk, and large coupling losses [12]. With the advancement of the EDFA, long distance transmission is no longer limited by attenuation; instead, it is limited by dispersion and non-linearity in optical fibers .EDFA can amplify different wavelengths simultaneously. The basic principle of EDFA is shown in the following figure.

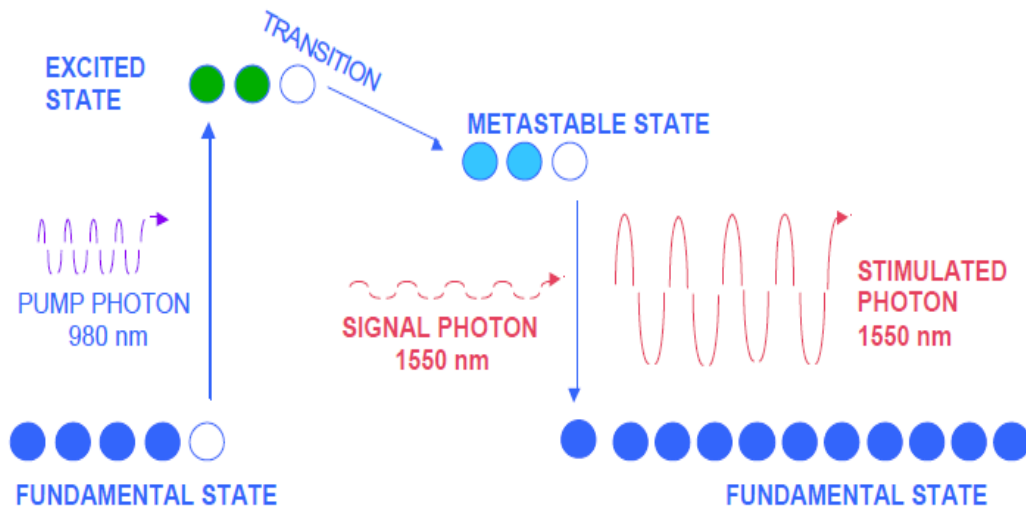


Figure 3.3-1: EDFA Working Principle

The electrons in the fundamental state absorb energy from a pumped photon and shifts to the excited state. In the excited state a transition occurs and the electrons move to the metastable state, which are then again coupled with photon of 1550 nm. As a result of this stimulated emission, we get the amplified signal at the output of the amplifier.

3.4 Amplifier Spontaneous Emission (ASE) Noise

During the process of amplification, some noise is also produced which is called the amplifier spontaneous emission noise. This noise originates during the transmission of electrons from metastable state to fundamental state.

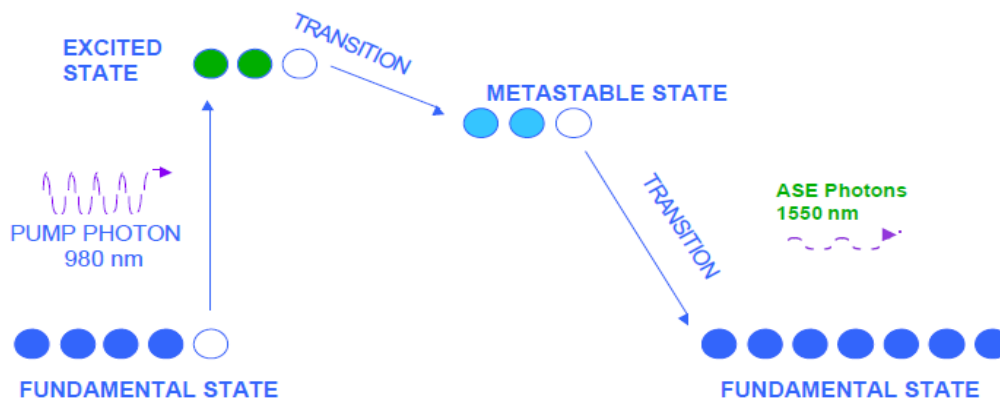


Figure 3.4-1: ASE noise

As shown in the figure above, there is some spontaneous recombination of holes and electrons or spontaneous transition of electrons from metastable state to fundamental state. During this spontaneous transition, photons are produced. These photons have random phase and amplitude. These random phased photons are coupled with the original signal and degrade the signal. This effect of degrading the signal is called Amplifier spontaneous noise (ASE) noise.

3.5 Effect of ASE Noise on BER

As the ASE noise distorts the input signal due to its random nature, the resulting BER is also degraded. A number of simulations were performed to evaluate this effect of ASE noise on the signal BER.

The signal flow followed for the evaluation of BER is shown in the following figure.

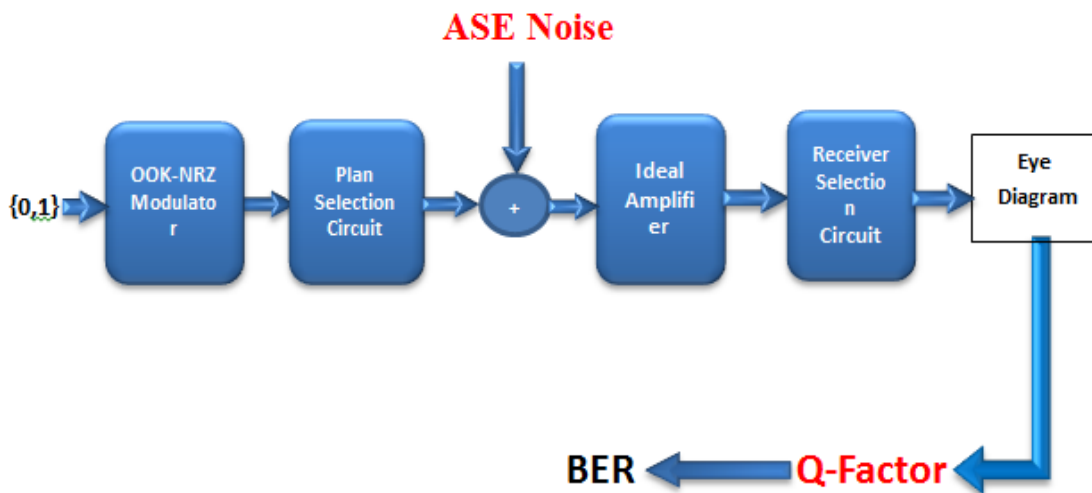


Figure 3.5-1: BER Evaluation Schematic (EDFA Noise)

Each signal transmitted at a specific wavelength has been filtered by the Plan Selection Circuit (PSC) transfer function and then selected by the corresponding Receiver Selection Circuit (RSC) transfer function. The eye diagram has been evaluated for each of the transfer functions resulting from all the TX-RX pair combinations.

3.6 Simulation Parameters

The above model has been simulated in MATLAB for 32 channels, spaced at 50 GHz. The channels are grouped into four groups of eight channels each. The electrical signal-to-noise (SNR) is given by the ratio of the signal power and noise power after electrical filtering with the same bandwidth as that of the PSC. The round-trip loss, α is considered to be zero. As a reference, in the Figure, the BER performance obtained in the ideal case, i.e., without signal distortions, is also reported.

3.7 Simulation Results

Figure 4.7-1 shows the BER performance versus the electrical SNR plots for all 32 channels. Figure 4.7-2 shows the best, the worse and the average BER performance versus electrical signal-to-noise ratio. From the curves we observe that the SNR loss of the average case with respect to that without (w/o) distortions varies between 6 dB, at BER=10⁻², and 8 dB, at BER=10⁻¹⁰. In the same range of BERs the SNR loss of the best channel with respect to that w/o distortions is comprised between 3.5 and 4 dB. The SNR gap between the best and the worse performance associated to Channel #10 and channel #7, respectively, varies between 4 dB, at BER=10⁻², and 5 dB, at BER=10⁻¹⁰.

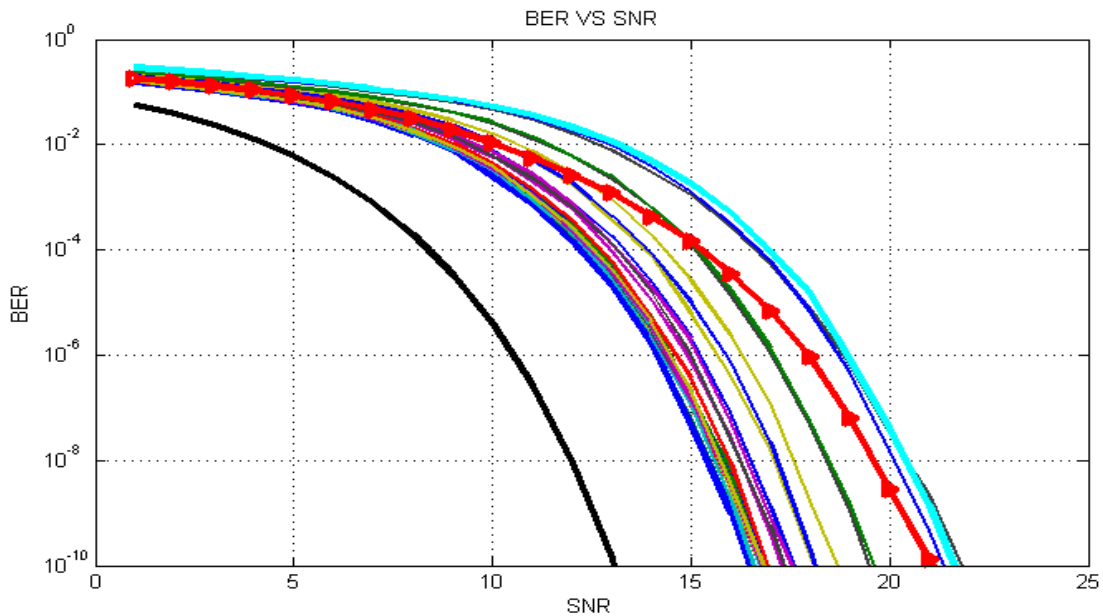


Figure 3.7-1: BER vs. SNR plot for all 32 channels at 50 GHz Spacing

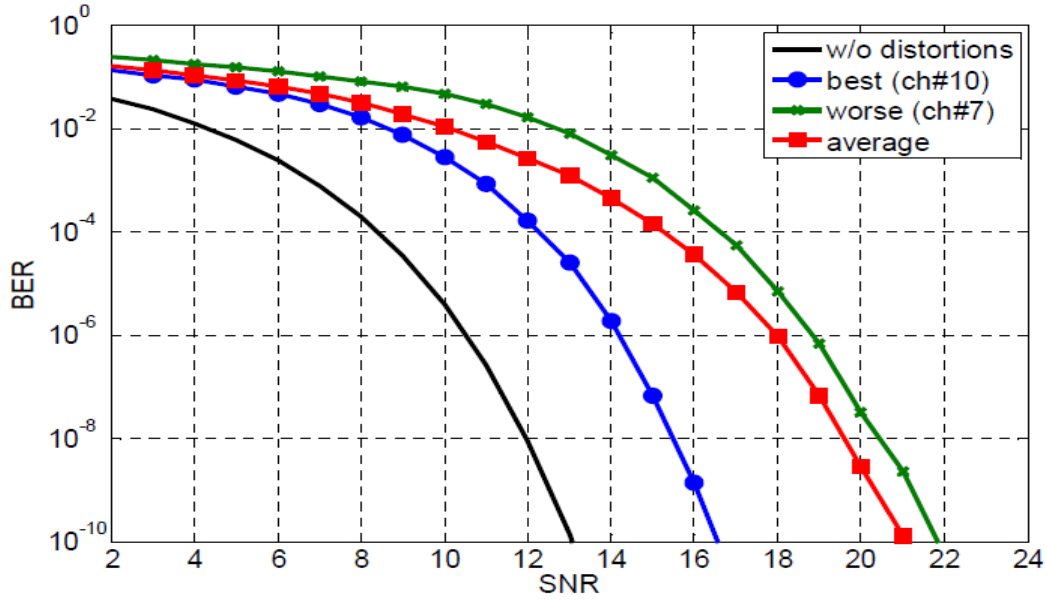


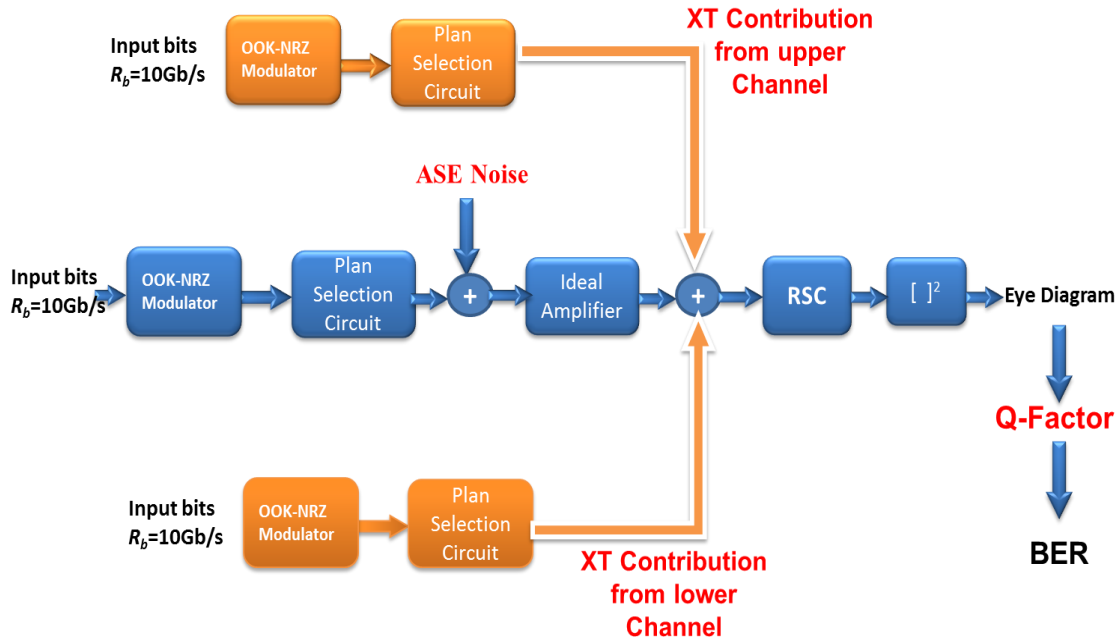
Figure 3.7-2: BER VS SNR - Best, Worst and Average Channels

3.8 Inter-Channel Interference (ICI)

Multiple Optical channels concurrently operate in close proximity on the same backplane to cope up with the spacing and miniaturization issues. This physical proximity and a wide range of different transmit and receive powers of neighboring channels, create challenging interference scenarios. Such interference often manifests itself as impulsive noise [13]. This impulsive noise from the neighboring channels above and below the channel of interest, contributes to the distortion of the transmitted signal. This section describes the effect of this Inter-channel interference on BER performance.

3.9 ICI Effect

ICI affects the transmitted signal by overlapping the signal start and end regions. The following figure 4.9-1 shows the scenario of this impulsive noise originated from the inter channel interference.



20

Figure 3.9-1: Inter-Channel interference

The figure above shows a visual illustration of the ICI in the ring resonator based optical backplane. The blue blocks indicate the channel of interest. The binary sequence of the transmitted message is modulated by passing through an OOK-NRZ modulator followed by the plane selection circuit which is basically the impulse response of the channel and then amplified by the EDFA which also add the ASE noise to the signal. The orange blocks indicate the cross talk (XT) or ICI contribution from above and below channels. A different signal is passed through the same path as that of the original message of interest. The three signals are combined after the EDFA and passed through the same Receiver Selection Circuit. The resulted signal is then passed through the ideal Photodetector which add no noise to the signal. From the simulated eye diagram the Q factor is then extracted, the same way as we did before. Finally the BER is obtained from the Q factor.

3.10 ICI effect on BER Performance

The above scenario is modeled in MATLAB to investigate that up to what extent it affects the BER performance.

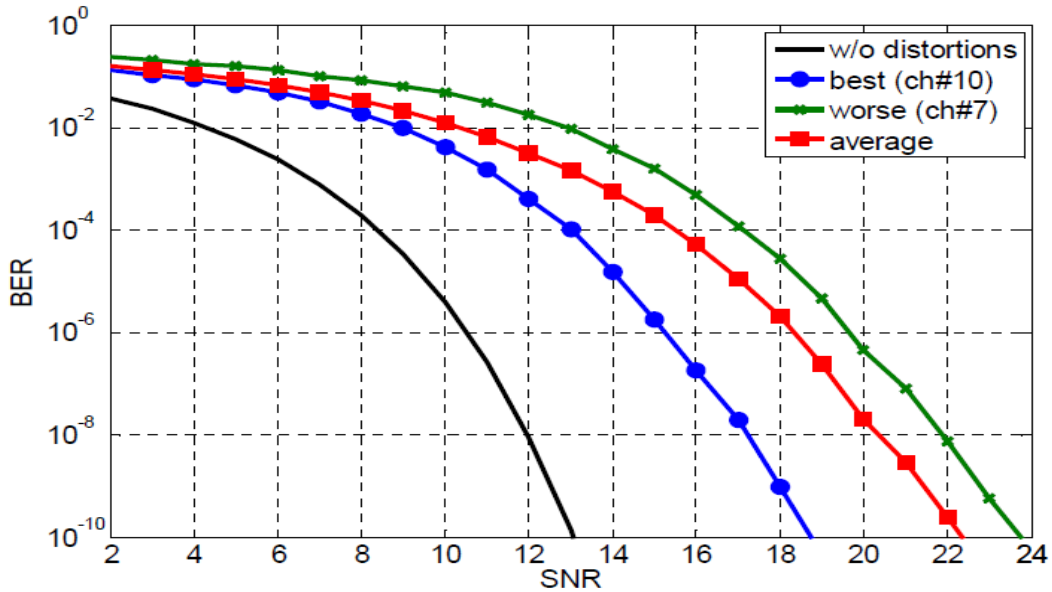


Figure 3.10-1: BER VS SNR - ICI effect

The figure 4.10-2 shows the BER VS SNR of the best, worst and average channel in case of ICI and EDFA noise. From the curve it can be depicted that the SNR loss of the average case with respect to that without (w/o) distortions varies between 6 dB, at BER=10⁻², and 9 dB, at BER=10⁻¹⁰. In the same range of BERs the SNR loss of the best channel with respect to that w/o distortions is comprised between 4 and 6 dB. The SNR gap between the best and the worse performance associated to Channel #10 and channel #7, respectively, varies between 4 dB, at BER=10⁻², and 5 dB, at BER=10⁻¹⁰.

The following figure compares the BER performance of the architecture when the signal is being interfered by ICI with the signal without affected by ICI.

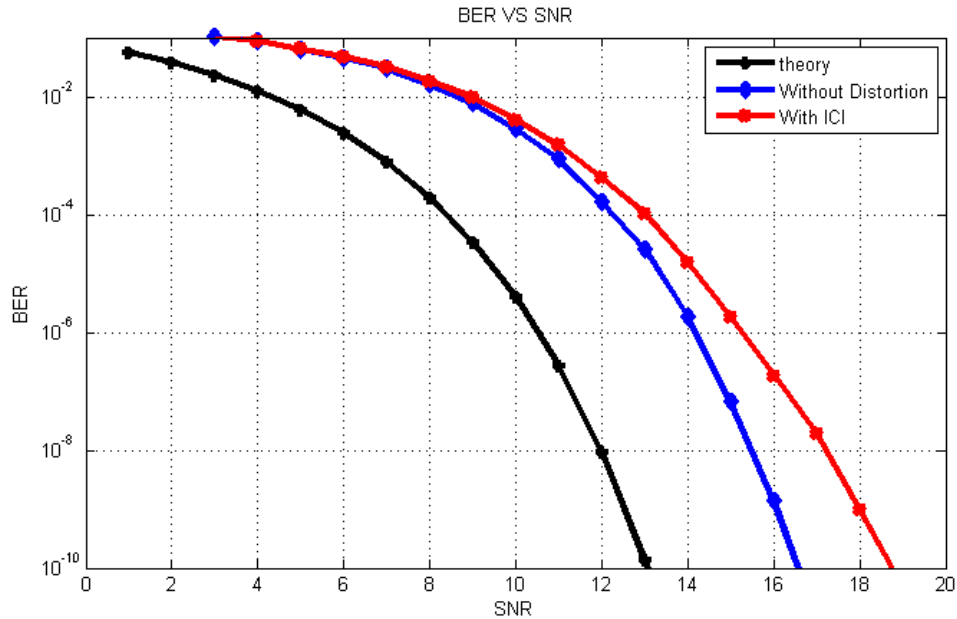


Figure 3.10-2: BER Performance comparison-With and Without ICI

From the curve we observe that in the situation where there is no Cross talk (XT) or ICI the SNR loss is 4dB at BER 10^{-2} and this loss of 4dB remains almost the same at BER 10^{-2} with respect to the theoretical BER. On the other hand if we observe the case in which the XT is introduced, the SNR loss at BER 10^{-10} increases up to 6 dB With respect to the theoretical BER curve. With respect to the BER performance of the channel without ICI or XT, the SNR loss at BER 10^{-10} is 2.5 dB. Thus it can be concluded that the XT introduced a degradation in the signal which resulted into an SNR loss of 2.5dB at BER 10^{-10} .

3.11 Photodetector Effect

Photodetector are used at the end of the architecture to convert the incoming signal in the form of light to electrical current when light energy impinges on it in the case of a binary 1 and no current for binary 0.

During this process of converting light into current some noise also originates. The main noises associated with Photodetector are Quantum (Shot) noise, Dark current noise and surface dark current. Due to these noises the signal quality degrades and as a result affects the BER.

As discussed previously the effect of EDFA noise and the degradation due to ICI, now the effect of Photodetector noise is also introduced into the process of evaluating the BER. The aim is to check the effect and the degradation in the BER due to this noise.

Photodetector can be modeled as the combination of the following three operations

1. Squaring
2. Noise addition
3. Passing through Low pass Filter

Figure 4.11-1 shows the equivalent model for the Photodetector.

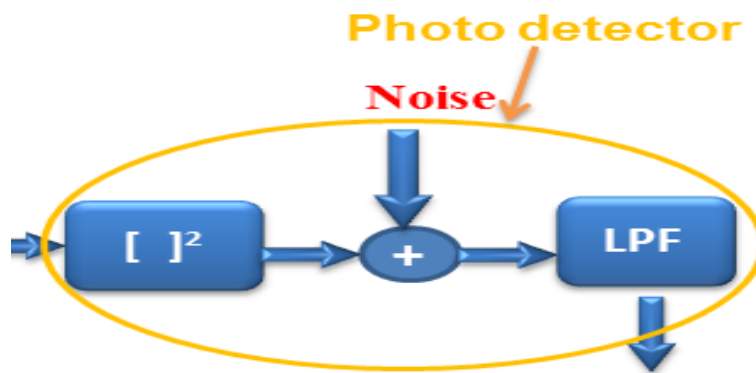


Figure 3.11-1: Photodetector Equivalent Model

Figure 4.11-2 shows the schematic for the evaluation of the BER in scenario in which Photodetector noise is introduced.

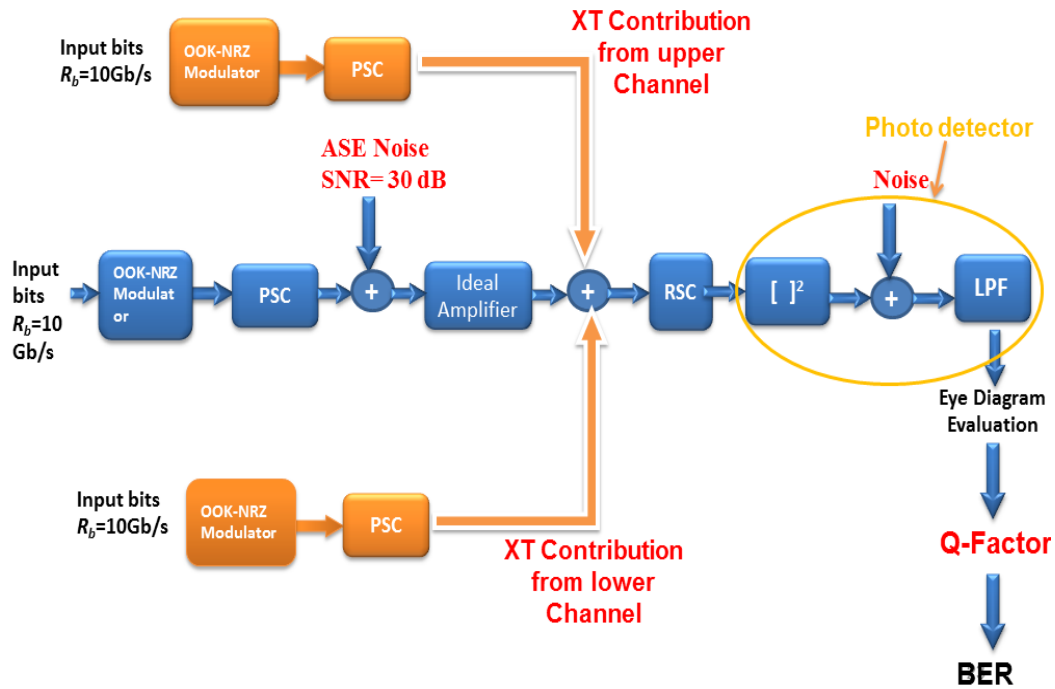


Figure 3.11-2: BER evaluation Schematic-Photodetector noise effect

In the above figure the signal after passing through the RSC is passed through the Photodetector which squares it and adds noise into it. After which the final operation is the low pass filtering. The signal is passed through low pass filter which is the final received signal available for analyzing.

In this particular scenario the noise due to EDFA is fixed at 30 db. It is because the EDFA has a fixed SNR in practical systems, so for this ring resonator based architecture a number of simulations were conducted to find the optimum SNR for EDFA. 30 dB was selected as the optimum. Actually the selected SNR for the EDFA is a little more than the optimum so as to be on the safe side.

The final BER is shown in the following figure which can be considered as the final overall performance considering all the possible noises which can be introduced by the ring resonator based optical backplane like EDFA noise, Inter channel Interference or XT and the Photodetector noise for the NRZ-OOK signal at 10Gb/s.

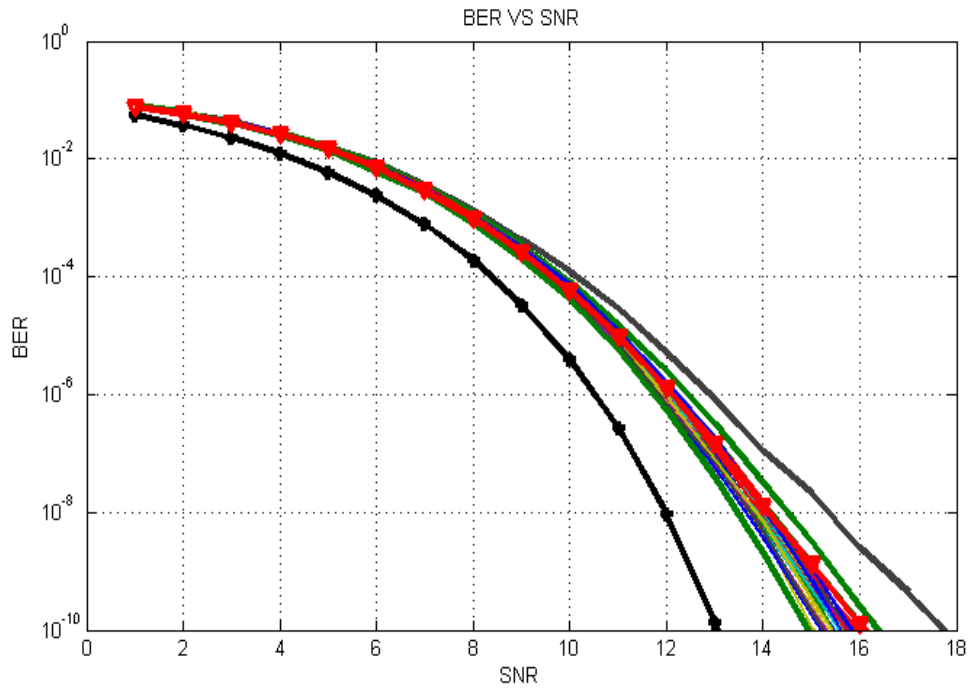


Figure 3.11-3: BER VS SNR – Overall architecture

From the figure it can be observed that the SNR loss at BER 10^{-2} is 2dB with respect to the theoretical curve and at BER 10^{-10} the SNR loss is almost 3 dB.

Overall if we observe the figure above it is clear that all the 32 channels curves are very close to each other which imply that all the channels performance is almost same.

3.12 Summary

The effect of Amplifier spontaneous noise (ASE), inter channel interference and Photodetector noise on the signal quality has been investigated and discussed in this chapter. The origin and source of the ASE noise is well explained. BER vs. SNR plots has been given and discussed in detail in scenarios of individual introduction of each type of noise. The combined effect of all these noises has also given and explained.

Temperature, Round trip Loss and Channel Spacing

4.1 Introduction

In practical scenarios, we have different variable parameters which we cannot avoid and these parameters have a great effect on the architecture. In order to find the feasibility of the architecture in real life in this chapter the effect of various parameters like temperature, round trip loss and channel spacing will be discussed. It will be investigated that how and up to which extent the architecture can tolerate the fluctuations in these parameters, and thus will determine the optimum and best practical conditions for the use of the architecture.

4.2 16 Channels at 50 GHz Spacing

The number of channels has been halved in this case, in order to find the variation caused in the BER when the spacing between the adjacent channels increases. All other parameters were kept the same, as was in the case of 32 channels i.e. the temperature and attenuation.

In this scenario from the curves we observe that the SNR loss of the average case with respect to that without (w/o) distortions varies between 3.5 dB, at BER=10⁻², and 4 dB, at BER=10⁻¹⁰. In the same range of BERs the SNR loss of the best channel with respect to that w/o distortions is comprised between 3 and 2.5 db. The SNR gap between the best and the worse performance associated to Channel #10 and channel #7, respectively, varies between 1 dB, at BER=10⁻², and 2 dB, at BER=10⁻¹⁰.

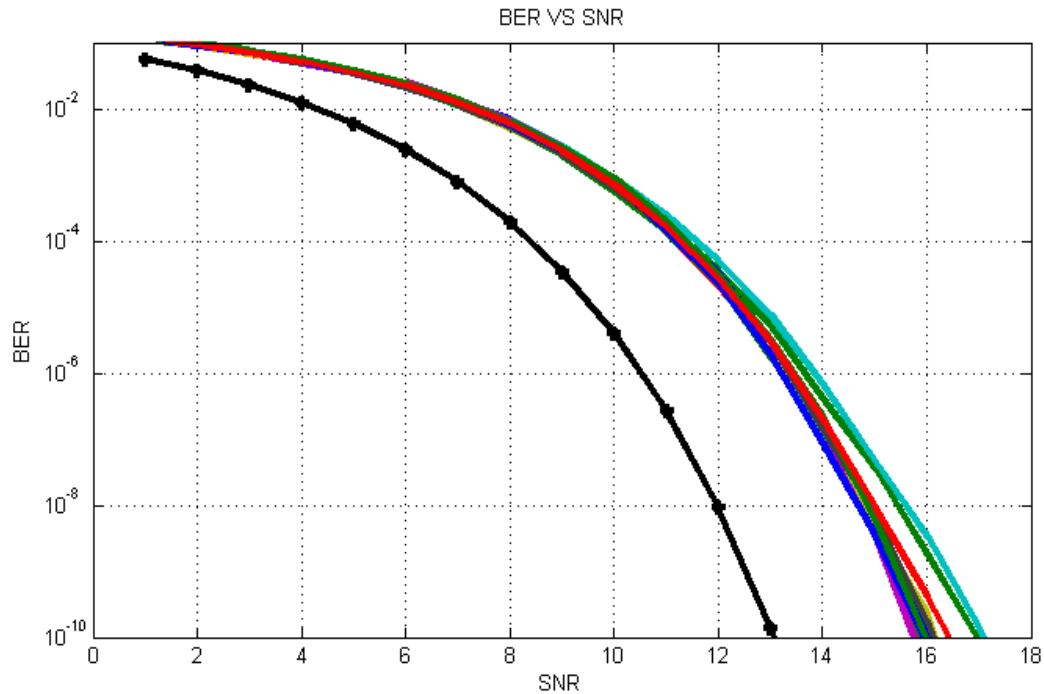


Figure 4.2-1: BER VS SNR plot for 16 channels at 100 GHz spacing

4.3 64 Channels at 25 GHz Spacing

To check the feasibility of the architecture at lower channel spacing, the number of channels has been increased to 64. These 64 channels, which are spaced at 25 GHz spacing, are grouped into 4 groups, each having 16 channels.

As shown in figure 5.3-1, we observe that the BER curve gives a noise floor at BER 10^{-2} . It shows that the architecture performance in the case of NRZ - OOK at 10 Gb/s for 64 channels is not that efficient as compared to the 16 and 32 Channels. In this case the signals are too close to each other which cause degradation of the signal in the optical fiber. Thus it is necessary to implement higher modulation schemes for the architecture to get efficient result and make the architecture perform efficiently at higher data rates.

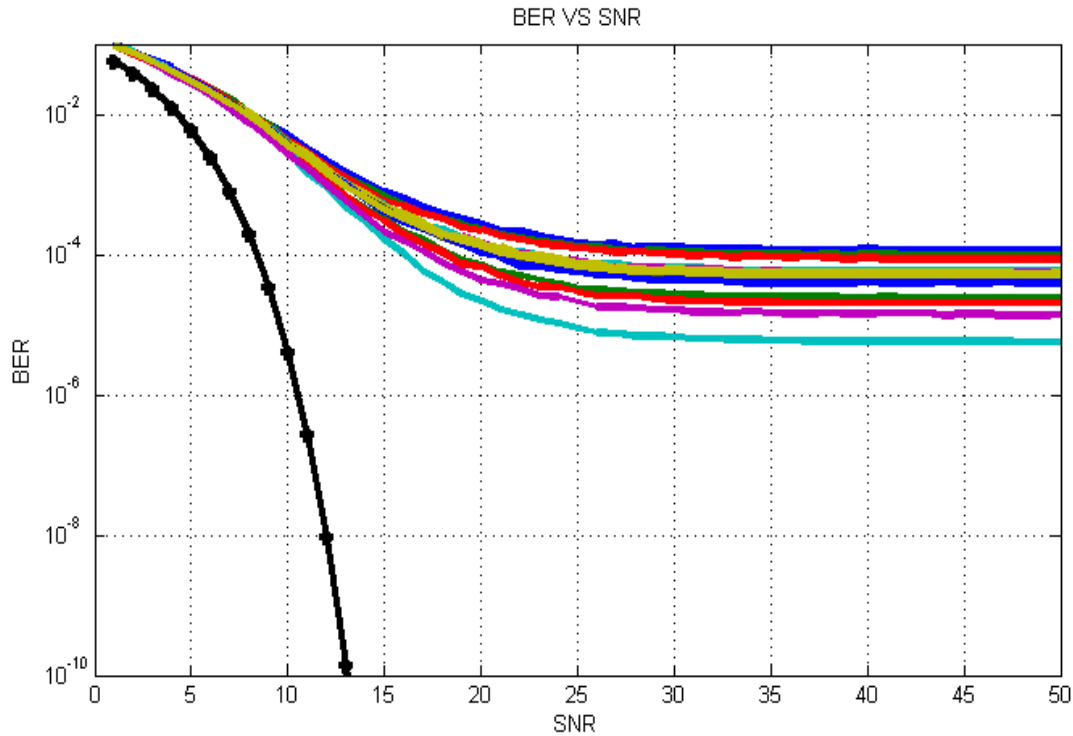


Figure 4.3-1: BER VS SNR plot case for 64 channels at 25 GHz spacing

4.4 Channel spacing Comparison

Figure 5.4-1 shows a comparison of all these three cases i.e. 32 channels at 50 GHz spacing, 16 channels at 100 GHz spacing and 64 channels at 25 GHz spacing for the best channel without considering the Photodetector noise.

From the figure it is depicted that as the spacing between the channels decreases, the SNR loss increases. Increasing the channel space from 25 GHz to 50 GHz, the SNR loss is less i.e. 1db at SNR 10^{-10} . But as we move from 50 GHz to 100 GHz, the SNR loss increases to 4.5 dB. From which we can derive that the increase in the loss of SNR with decreasing the channel spacing is exponential.

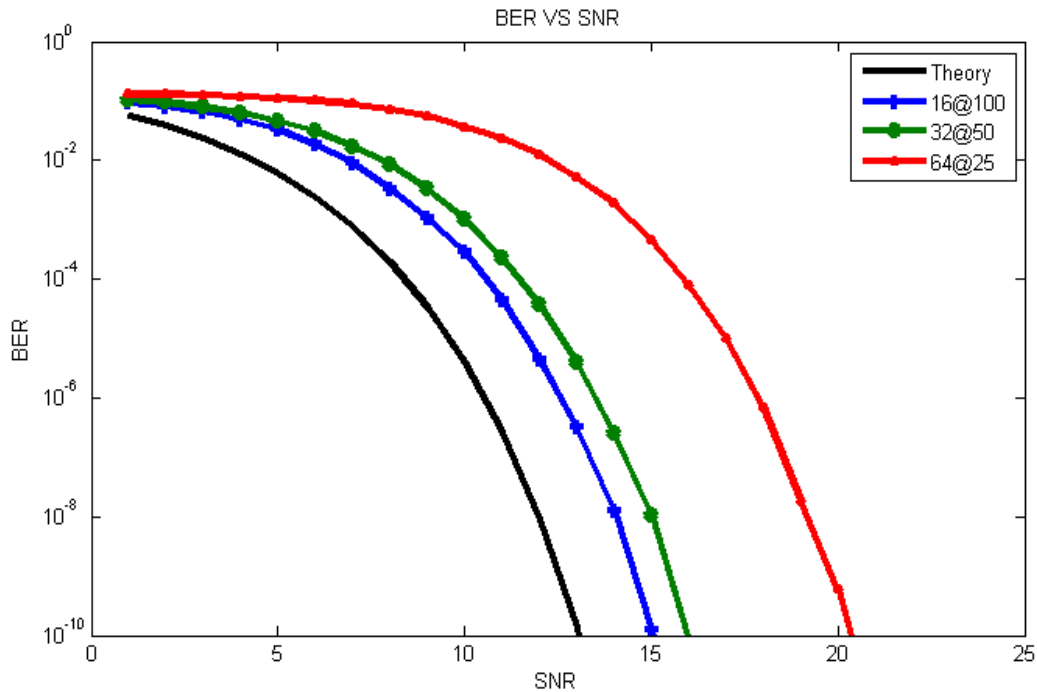


Figure 4.4-1: Comparison of 25, 50 and 100GHz channel spacing without Photodetector noise

Now consider the case where the effect of the Photodetector noise is also included for analyzing the effect of channel spacing on the ring resonator based optical backplane architecture.

Figure 5.4-2 shows a comparison of the 25GHz, 50GHz and 100 GHz spacing effect on the overall BER curve. It can be observed that performance is good for 100 GHz and 50 GHz spacing but as we decrease the spacing to 25GHz, we get an error floor of BER at 10^{-5} . From which we can conclude that the system is intolerant to channel spacing, less than 50 GHz. Thus to get excellent performance from this ring resonator based optical backplane architecture, this limitation of channel spacing should be kept in mind under the same conditions i.e. using NRZ – OOK modulation scheme at 10 Gb/s. For using the system for higher data rate and with small spacing, we will have to use higher modulation schemes like BPSK, Quadrature Amplitude Modulation (QAM) etc.

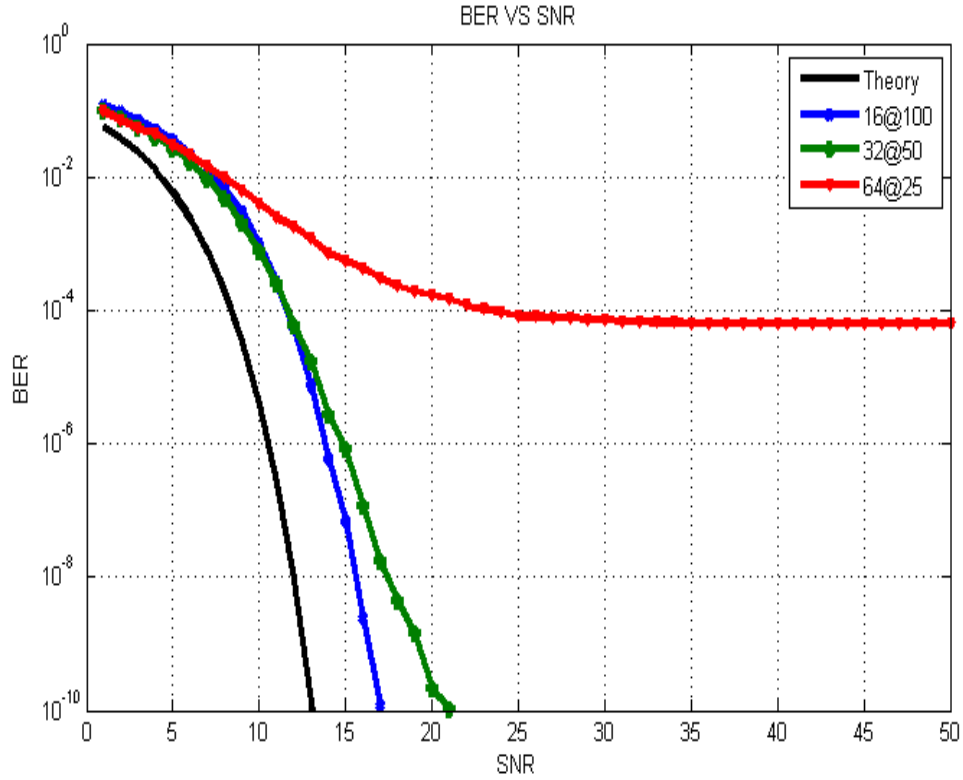


Figure 4.4-2: Comparison of 25, 50 and 100GHz channel spacing with Photodetector noise

4.5 Effect of Temperature

The change in refractive index of a material as a function of its change in temperature is known as the thermo-optic effect:

$$\Delta n_{eff} = K\Delta T$$

Where n_{eff} represents the variation on the effective refractive index, T is the variation in temperature to which a waveguide undergoes. K is the thermo-optic coefficient and it has been known for some time that this effect is quite large in silicon, that is $10^{-4} \text{ } ^\circ\text{C}^{-1}$ [14]. If we relate Δn_{eff} to Δf by

$$\Delta f = \frac{K\Delta T f_0}{n_{eff}}$$

That is the resonant frequency drifting from f_0 , we obtain that $\Delta T = 1^\circ\text{C}$ corresponds to 10 GHz frequency shift (silicon). This effect has been widely and successfully exploited to realize devices that work on the principle of phase modulation. As a matter of fact, a design issue is to cope with unintentional waveguide temperature variation. The impact of such type of temperature variation on the overall BER of the system has investigated when a thermal variation within the range ± 0.5 , ± 1 and $\pm 1.5^\circ\text{C}$ is applied to any ring resonator of the architecture with uniform probability distribution.

Figure 5.5-1 shows the BER for 32 channels spaced at 50 GHz when the temperature is varied by 0.5°C i.e. for 0, 0.5, 1 and 1.5°C . It is evident the SNR loss for 0.5°C at BER 10^{-2} is 2 dB with respect to the theoretical BER and at 10^{-10} the SNR loss is 2.5dB. For temperature increase of 1°C and 1.5°C the performance is almost same i.e. 3dB and 4dB within the same range of BER. For temperature increase of 1.5°C the SNR loss is 3dB at BER 10^{-2} and 5dB at BER 10^{-10} . Thus it is clear that the architecture is sensitive to the temperature rise greater than 1.5°C .

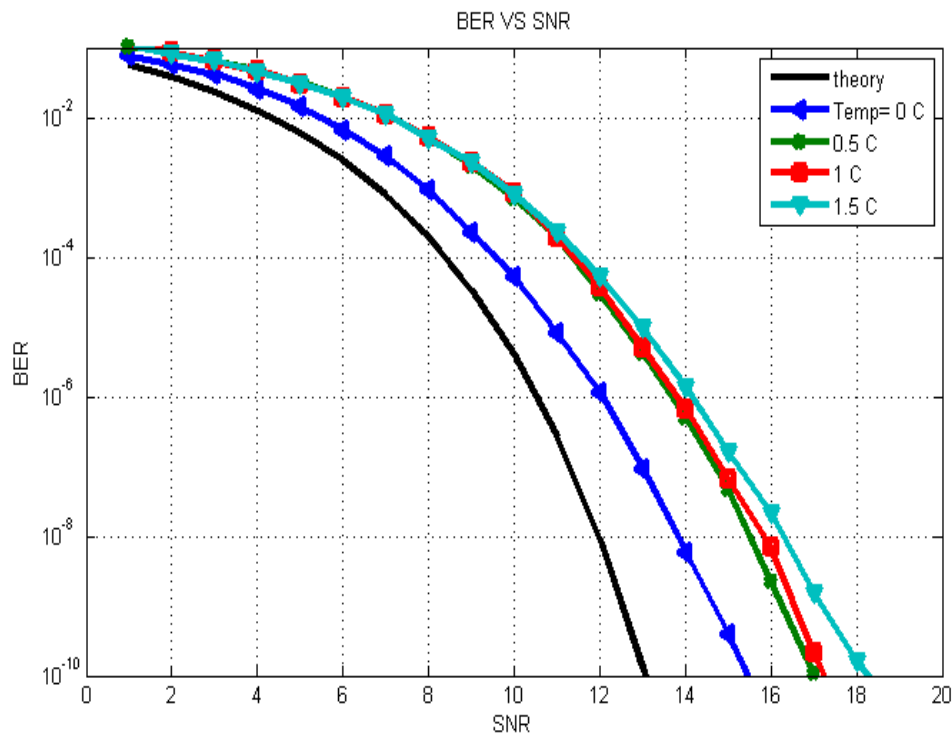


Figure 4.5-1: BER vs. SNR- Temperature Effect

4.6 Round trip Loss

The propagation of light in fiber optic is not 100% efficient. As light propagates through the fiber, it losses some power over distance. This loss is dependent on fiber material properties and wavelength of the signal used. This loss of power attenuates the signal. For different materials there is a specific attenuation or round-trip loss at specific wavelength.

The impact of round-trip losses on the ring transfer function is remarkable. As the round-trip losses increases the drop insertion loss increases and we get an error floor of BER. Also when many ring resonators are cascaded to increase the bandwidth, the filter becomes less selective due to which the performance degraded and cross talk (XT) is introduced in the channels. This XT effect cannot be mitigated by the Receiver filter, as it is also affected by the round-trip loss.

Fig 5.6-1 reports the best and the worst performance associated to channel #10 and channel #7, respectively, for increasing values of the round-trip loss $\alpha = 0, 0.2, 0.4, 0.6, 0.8, 1$. From the figure we observe that for a given value of α SNR gap between the best and the worse channel is approximately always the same. Moreover, an SNR loss of approximately 5 dB can be observed between $\alpha = 0$ and $a = 1$.

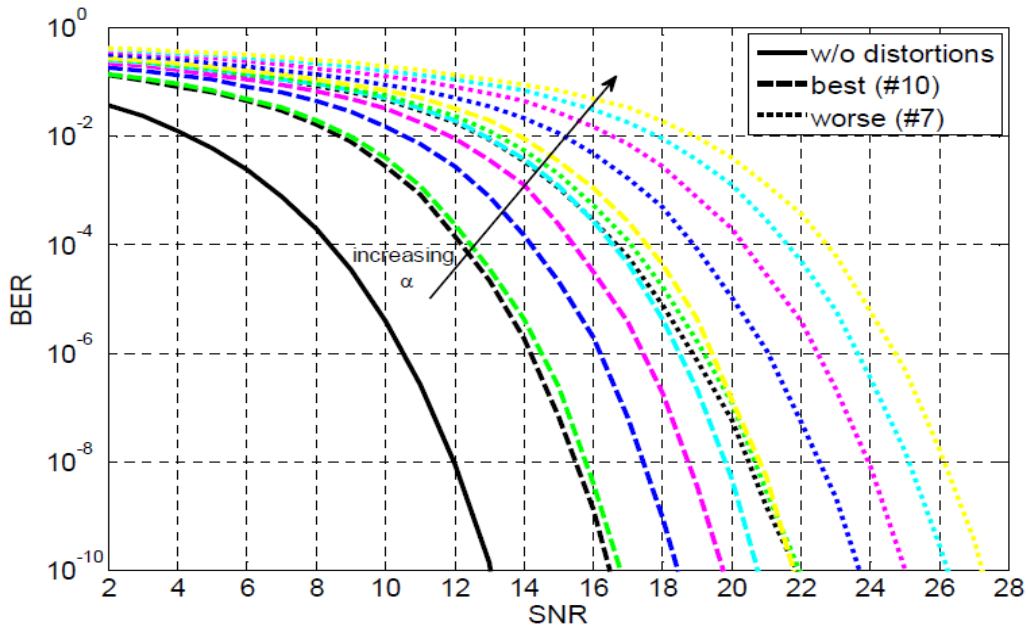


Figure 4.6-1: BER vs. SNR for transmission at 10 Gb/s of 32 NRZ-OOK channels with increasing round-trip losses $\alpha = 0, 0.2, 0.4, 0.6, 0.8, 1$.

In Figure 5.6-2 the effect of XT on the best and the worse performance is reported for increasing values of the round-trip losses $\alpha = 0, 0.2, 0.4, 0.6, 0.8, 1$. In contrast to the analogous situation without XT considered in Figure 5.6-1, in this case we observe that for the values of α equal to 0.6, 0.8 and 1 the BER presents an error floor. This effect arises because the presence of some configurations of interference that causes the closure of the eye even in the situation where noise is absent. By comparing the curves reported in Figures 5.6-1 and 5.6-2 at a given BER it is possible to evaluate the degradation introduced by XT for a fixed value of α .

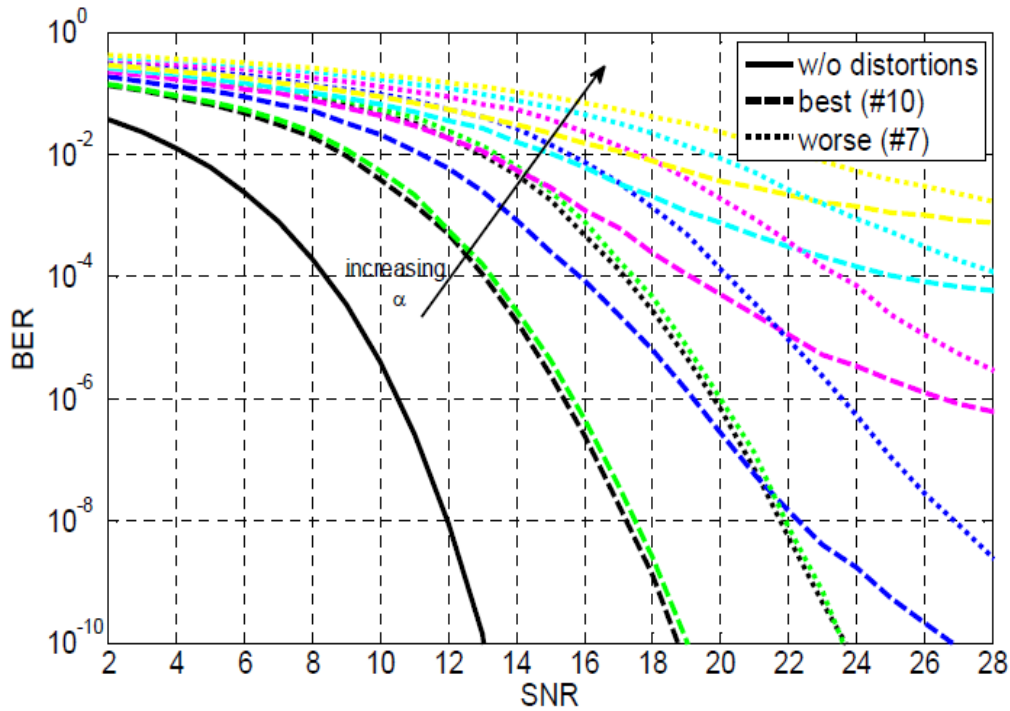


Figure 4.6-2: BER vs. SNR for transmission at 10 Gb/s of 32 NRZ-OOK channels with increasing round-trip losses $\alpha = 0, 0.2, 0.4, 0.6, 0.8, 1$ in presence of XT

It is worth observing that for input signals with rates higher than 10 Gb/s, *i.e.*, 40, 100, and 160 Gb/s an increase of modulation order is required in order to satisfy the bandwidth limitation imposed by the optical filtering. As is well known, high order modulation formats require coherent demodulation and are more sensitive to signal distortions introduced by optical filters and XT. Therefore, in order to achieve a performance that is comparable with that of 10 Gb/s transmission an appropriate signal processing is required.

4.7 Summary

The architecture has been analyzed in different scenarios by changing the physical parameters like temperature, channel spacing and round trip losses. BER vs. SNR plots are given to show the effect of these parameters on the signal quality. It has been depicted from the results that the architecture is sensitive to temperature change greater than 1.5°C and round trip loss greater than 0.4 dB. The architecture is also very sensitive to channel spacing. At 25 GHz spacing a noise floor has been observed at BER 10^{-4} using NRZ-OOK modulation scheme.

Conclusion and Future Work

A new RR-based switching fabric has presented and a novel approach to assess architecture performance in terms of Bit Error Rate. Our BER analysis allows us to accurately capture the impact of each design issue with respect to the ideal scenario. This capability is not achievable in power budget and XT power penalty evaluations. In this work, the OI architecture is analyzed in terms of optical performance parameters and signal distortions introduced by the filtering operations performed by PSC and corresponding RSC for a given value of the wavelength of the input signal. Moreover the effect of change in temperature, round-trip loss and channel spacing has also been investigated. From the observation of the eye diagrams for all the TX-RX pairs in case of OOK-NRZ transmission at 10 Gb/s, performance analysis has been worked out by estimating the BER both without and with XT vs. SNR of the proposed architecture.

This work can be extended by implementing higher modulation schemes like QAM etc. Also the data rate can be increased and introducing the matching filter to reverse the effect of the PSC and the RSC to make the system efficient.

References

- [1] Giuseppe Rizzelli, Domenico Siracusa, Guido Maier, Maurizio Magarini, Andrea Melloni, "Performance of Ring-Resonator Based Optical Backplane in High Capacity Routers", ICTON 2013, Austria
- [2] S. K. Korotky: "Traffic trends: Drivers and measures of cost-effective and energy-efficient technologies and architectures for backbone optical networks", in *Proc. OFC*, Los Angeles, CA, Mar. 2012, paper OM2G.1.
- [3] A. Bianco, E. Carta, D. Cuda, J. Finochietto, and F. Neri; An optical interconnection architecture for large packet switches; *Proc. ICTON 2007*, Rome, Italy.
- [4] N. McKeown "A fast switched backplane for a gigabit switched router; *Business Communications*" Review, vol. 27, no.12, Dec. 1997.
- [5] Seventh Framework Programme; D25.2: Report on Y1 and updated plan for activities; Building the Future Optical Network in Europe (BONE), Dec. 2009.
- [6] Iftikhar.Rasheed, Muhammad Farrukh Amin. Sial, Khawaja Salman. Ali, and Tariq.Mehboob Evaluation of Optical Receiver Sensitivity-Bit Error Rate (BER)/Q factor, International Conference on Computer and Communication Technologies (ICCCCT'2012) May 26-27, 2012 Phuket
- [7] Optical Signal-to-Noise Ratio and the Q-Factor in Fiber-Optic Communication Systems, Application Note: HFAN-9.0.2 Rev.1; 04/08
- [8] René-Jean Essiambre, *Senior Member, IEEE, Fellow, OSA*, Gerhard Kramer, *Fellow, IEEE*, Peter J. Winzer, *Fellow, IEEE*, Gerard J. Foschini, *Fellow, IEEE*, and Bernhard Goebel, *Student Member, IEEE*, Capacity Limits of Optical Fiber Networks, *JOURNAL OF LIGHTWAVE TECHNOLOGY*, VOL. 28, NO. 4, FEBRUARY 15, 2010
- [9] John D. Downie, "Relationship of Q Penalty to Eye-Closure Penalty for NRZ and RZ Signals With Signal-Dependent Noise", *journal of light wave technology*, vol. 23, no. 6, June 2005
- [10] Mobilon, E. CPqD Telecom & IT Solutions, Campinas ; de Barros, M.R.X. "Low cost eye diagram reconstruction and morphological analysis for optical network performance monitoring using digital signal processing techniques" *Telecommunications Symposium*, 2006 International, Fortaleza, Ceara
- [11] A. K. Jaiswal, Anil Kumar, Santosh Tripathi, Amarendra Kumar Chaudhary, "To Study the Effect of BER and Q-factor in Intersatellite Optical Wireless Communication System" *IOSR Journal of Electronics and Communication Engineering (IOSR-JECE)* ISSN: 2278-2834, ISBN: 2278-8735. Volume 3, Issue 4 (Sep-Oct. 2012), PP 19-21
- [12] Tuan Nguyen Van , Vu Le Tuan ; Khoa Ho Van "Investigating performance of radio over fiber communication system using different silica-doped materials, EDFA and coherent receiver",
- [13] F Leferink, F Silva, J Catrysse, S Batterman, V Beauvois, A Roc'h, Man-made noise in our living environments. *Radio Sci Bull.* 334, 49–57 (2010)